
Multi-Domain Empirical Bayes for Linearly-Mixed Causal Representations

Bohan Wu¹Julius von Kügelgen²David M. Blei¹¹ Department of Statistics, Columbia University, USA² Seminar for Statistics, ETH Zürich, Switzerland

Abstract

Causal representation learning (CRL) aims to learn low-dimensional causal latent variables from high-dimensional observations. While identifiability has been extensively studied for CRL, estimation has been less explored. In this paper, we explore the use of empirical Bayes (EB) to estimate causal representations. In particular, we consider the problem of learning from data from multiple domains, where differences between domains are modeled by interventions in a shared underlying causal model. Multi-domain CRL naturally poses a simultaneous inference problem that EB is designed to tackle. Here, we propose an EB f -modeling algorithm that improves the quality of learned causal variables by exploiting invariant structure within and across domains. Specifically, we consider a linear measurement model and interventional priors arising from a shared acyclic SCM. When the graph and intervention targets are known, we develop an EM-style algorithm based on causally structured score matching. We further discuss EB g -modeling in the context of existing CRL approaches. In experiments on synthetic data, our proposed method achieves more accurate estimation than other methods for CRL.

arising from sparse interventions in an underlying causal model [32, 33], while the remaining causal mechanisms and the measurement process are shared across domains.

Most prior work on CRL, including in the multi-domain setting, has focused on the question of *identifiability* [2, 7, 23, 44, 49, 51, 54, 58, 59]: under what conditions and up to what ambiguities can the latent causal variables provably be recovered at the population level, i.e., in the infinite-data regime? In this paper, we focus on the *estimation problem*. How can we learn causal representations from finite samples of noisy measurements?

CRL naturally amounts to a *simultaneous inference* problem: each observation has its own local latent variable, yet these variables follow a shared distribution induced by the underlying causal model. In the multi-domain CRL setting, such information sharing occurs within and across domains, since the measurement process and parts of the causal model are assumed to remain invariant.

In statistics, the idea of *empirical Bayes* (EB) offers an elegant solution to the problem of simultaneous inference of many local latent variables [15, 21, 38, 55]. The canonical EB setup assumes all local latent variables are i.i.d. according to a shared and unknown prior, and then solves the problem of simultaneous inference via shrinkage [22]. Multi-domain CRL provides a novel version of this problem, where the local variables are the latent causal variables, and the domains exhibit structured heterogeneity through sparse interventions. We develop EB methods for this CRL setting.

1 INTRODUCTION

Causal representation learning (CRL) seeks to recover low-dimensional latent causal variables from high-dimensional realizations [1, 29, 39]. Since this task is highly challenging in general [19, 26], a common approach is to leverage heterogeneous (non-i.i.d.) data as a learning signal [20, 50]. A central idea is that invariances under heterogeneity can reveal causal information [57]. A prominent example is grouped data from different environments or domains. From a causal perspective, such *multi-domain* data is typically viewed as

Overview and contributions. In this work, we adopt a probabilistic perspective on CRL with noisy measurements and focus on finite-sample estimation via EB. We first develop the connection between CRL and EB at the conceptual level of modeling principles (§ 2), and then study a concrete class of noisy multi-domain latent causal models (§ 3). Specifically, we consider linear measurement models (§ 3.1) with interventional priors induced by an acyclic latent SCM with known causal graph and intervention targets (§ 3.2).

We then explore EB estimation for this model class. Under an orthogonality condition on the mixing matrix, projecting observations yields a normal means model, which facilitates an EM-style f -modeling EB approach (§ 4), wherein posterior denoising can be expressed through Tweedie’s formulas in terms of the score of the marginal distribution. We leverage the causal graph structure to parameterize and efficiently estimate this score across domains (§ 5), yielding an iterative algorithm (Alg. 1) that alternates score estimation, Tweedie updates for denoising latents, and EM updates for the mixing matrix and noise variance. We then discuss the g-modeling EB approach and establish connections to existing methods that fall into this category (§ 6). Through empirical studies on synthetic interventional data (§ 7), we demonstrate that CRL f -modeling improves latent recovery relative to natural baselines and provides stable performance across domains.

Notation. We write column vectors in bold lowercase (e.g., $\mathbf{x} \in \mathbb{R}^d$), with x_i denoting the i^{th} entry, and matrices in bold uppercase (e.g., $\mathbf{A} \in \mathbb{R}^{d \times k}$), with \mathbf{A}_i denoting the i^{th} row and \mathbf{A}_{ij} the $(i, j)^{\text{th}}$ entry. Let $\mathcal{O}^{d \times k}$ denote the Stiefel manifold of $d \times k$ matrices with orthonormal columns. For $n \in \mathbb{N}$, define $[n] := \{1, \dots, n\}$. The set $\mathcal{P}(\Omega)$ stands for the set of probability measures over Ω . In a directed graph, $\text{pa}(j)$ and $\text{ch}(j)$ denote the parents and children of node j . Partial derivatives w.r.t. the j^{th} argument are denoted by ∂_j and gradients by ∇ . If $\mathbf{x} \in \mathbb{R}^d$, $\mathbf{x} \odot \mathbf{x}$ denotes the vector of element-wise squares, i.e., $\mathbf{x} \odot \mathbf{x} = (x_1^2, \dots, x_d^2)^\top$.

2 CAUSAL EMPIRICAL BAYES

Consider M domains, each of which is characterized by a fixed observed action or perturbation label $\mathbf{a}_e \in \mathcal{A} := \{\mathbf{a}_1, \dots, \mathbf{a}_M\} \subseteq \mathbb{R}^{d_A}$. For each $\mathbf{a}_e \in \mathcal{A}$, we have access to an i.i.d. sample of realizations $\mathbf{x} \in \mathbb{R}^{d_x}$ from an unknown population distribution $p^*(\mathbf{x} | \mathbf{a}_e)$, i.e., we observe data

$$\mathcal{D} = \left(\left((\mathbf{x}_{ei})_{i=1}^{N_e}, \mathbf{a}_e \right)_{e=1}^M \right), \quad (2.1)$$

where $(\mathbf{x}_{ei})_{i=1}^{N_e} \stackrel{\text{iid}}{\sim} p^*(\mathbf{x} | \mathbf{a}_e)$.

The distributions $\{p^*(\mathbf{x} | \mathbf{a})\}_{\mathbf{a} \in \mathcal{A}}$ can be thought of as *interventional* distributions, in the sense that each \mathbf{a}_e contains (partial) information on which intervention or experiment was performed in domain e .

To model $p^*(\mathbf{x} | \mathbf{a})$, we use a latent variable model with local latents $\mathbf{z} \in \mathbb{R}^{d_z}$, one for each \mathbf{x} . In the context of single-cell measurements \mathbf{x} , these latent variables could represent, e.g., gene programs or clusters of proteins. Importantly, we assume that \mathbf{z} fully mediates the effect of \mathbf{a} on \mathbf{x} , so that the relationship between \mathbf{z} and \mathbf{x} (e.g., the measurement process) is invariant across domains while only the distribution of \mathbf{z} may change, see Fig. 1. We formalize this as follows.

Assumption 2.1 (Causal empirical Bayes). For all $\mathbf{a} \in \mathcal{A}$, there exists an interventional prior $p^*(\mathbf{z} | \mathbf{a})$ s.t. the true

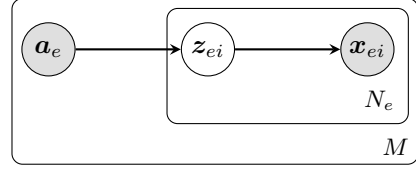


Figure 1: **Assumed graphical model.** Shaded nodes are observed, white nodes are latent. The inner plate is over realizations $i = 1, \dots, N_e$, the outer over domains $e = 1, \dots, M$.

interventional marginal $p^*(\mathbf{x} | \mathbf{a})$ can be expressed as

$$p^*(\mathbf{x} | \mathbf{a}) = \int_{\mathbb{R}^{d_z}} p^*(\mathbf{x} | \mathbf{z}) p^*(\mathbf{z} | \mathbf{a}) d\mathbf{z}. \quad (2.2)$$

We refer to Thm. 2.1 as the *causal empirical Bayes assumption*, as it connects the Bayesian latent variable model on the RHS to the true causal data-generating process on the LHS. Accordingly, we refer to \mathbf{z} as the *latent causal variables*. Eq. (2.2) admits two complementary interpretations. Read from right to left, it implies that the probabilistic model $\mathbf{z} \sim p^*(\mathbf{z} | \mathbf{a})$ and $\mathbf{x} \sim p^*(\mathbf{x} | \mathbf{z})$ is a *well-specified* generative model for the true interventional distribution $p^*(\mathbf{x} | \mathbf{a})$. Read from left to right, on the other hand, it suggests an *empirical Bayes* interpretation: given the true marginal $p^*(\mathbf{x} | \mathbf{a})$ and the likelihood $p^*(\mathbf{x} | \mathbf{z})$, we may infer the true prior $p^*(\mathbf{z} | \mathbf{a})$. In this view, the prior can be learned from the data using a g-modeling approach [14] or indirectly using f -modeling [12, 38], see § 4 for details.

Our target of inference is the posterior of the latent causal variables:

$$p^*(\mathbf{z} | \mathbf{x}_{ei}, \mathbf{a}_e) \propto p^*(\mathbf{z} | \mathbf{a}_e) p^*(\mathbf{x}_{ei} | \mathbf{z}). \quad (2.3)$$

Here, both the measurement model $p^*(\mathbf{x} | \mathbf{z})$ and the domain-specific priors $p^*(\mathbf{z} | \mathbf{a}_e)$ are unknown quantities.

3 CRL MODEL CLASS

We now describe the assumptions we place on the measurement model (§ 3.1) and domain-specific priors (§ 3.2).

3.1 LINEAR GAUSSIAN MEASUREMENT MODEL

We focus on the setting in which the measurement model is linear with additive, zero-mean, isotropic Gaussian noise.

Assumption 3.1 (Linear Gaussian measurement model). For all $e \in [M]$, $i \in [N_e]$, the generative process is

$$\begin{aligned} \mathbf{z}_{ei} &\sim p^*(\mathbf{z} | \mathbf{a}_e), \\ \mathbf{x}_{ei} &= \mathbf{A}^* \mathbf{z}_{ei} + \boldsymbol{\varepsilon}_{ei}, \quad \boldsymbol{\varepsilon}_{ei} \sim \mathcal{N}(\mathbf{0}, \sigma^{2*} \mathbf{I}_{d_x}), \end{aligned} \quad (3.1)$$

for some unknown true mixing or loading matrix $\mathbf{A}^* \in \mathbb{R}^{d_x \times d_z}$ and unknown true noise variance σ^{2*} .

Consider a single domain ($M = 1$) with equal latent and observed dimensionality ($d_X = d_Z$) and no mixing ($\mathbf{A} = \mathbf{I}_{d_X}$). In this setting, the model in (3.1) corresponds to (a multi-variate version of) the classical empirical Bayes normal means model [38], which aims to recover the unknown mean $z_i = \mathbb{E}[x_i]$ for each observation x_i , under the assumption that the means are drawn from a single shared prior $z_i \sim g$. The single-domain setting with $d_X > d_Z$ and *unknown* \mathbf{A} constitutes a generalization of this classical setting, which is related to probabilistic PCA [45].¹

For multiple domains ($M > 1$), Thm. 3.1 generalizes the classical setting, where each domain has a possibly different prior $z_{ei} \sim g_e := p^*(z | \mathbf{a}_e)$. That is, an empirical Bayes setup plays out in each domain. However, there is not only information sharing *within* domains, through the shared priors g_e , but also *across* domains, through the shared measurement model and shared causal structure among the domain-specific priors. This raises the following central questions, which we seek to answer in the present work.

How can the assumed multi-domain structure be leveraged to accurately estimate the shared measurement model and the latent variables? Can empirical Bayes estimation be generalized to the model from (3.1)?

Rather than study these questions for arbitrary nonparametric priors g_e , we place additional structure on the domain-specific priors to incorporate the available information in the form of the observed action labels \mathbf{a}_e .

3.2 INTERVENTIONAL STRUCTURAL PRIORS

To set the interventional priors $\{p^*(z | \mathbf{a}_e)\}_{\mathbf{a}_e \in \mathcal{A}}$, we adopt the structural causal model framework [SCM; 31, 34] to describe the causal relations among latent variables.

Definition 3.2 (Acyclic SCM). Let $\mathbf{z} = (z_1, \dots, z_d)$ denote endogenous (causally determined) variables, and let $\mathbf{u} = (u_1, \dots, u_d)$ denote exogenous (noise) variables. A *structural causal model* (SCM) $\mathcal{M} = (\mathbf{F}, \rho_{\mathbf{u}})$ over \mathbf{z} consists of: (i) a collection of d structural assignments:

$$\mathbf{F} = \left\{ z_j := f_j \left(\mathbf{z}_{\text{pa}(j)}, u_j \right) \right\}_{j=1}^d, \quad (3.2)$$

where each f_j is a measurable function mapping the values of the parents, or direct causes, $\mathbf{z}_{\text{pa}(j)}$ of z_j , and noise u_j to the value of z_j ; and (ii) a distribution over the exogenous variables: $\mathbf{u} \sim \rho_{\mathbf{u}}$. The *causal graph* \mathcal{G} induced by \mathcal{M} , given by the directed graph with nodes $\{1, \dots, d\}$ and edges $\mathcal{E} = \{(k, j) \mid k \in \text{pa}(j)\}$, is assumed acyclic. The *distribution* $p_{\mathcal{M}}(\mathbf{z})$ induced by \mathcal{M} is given by the pushforward of $\rho_{\mathbf{u}}$ under the structural assignment map \mathbf{F} .

¹Without additional assumptions on \mathbf{A}^* and $p^*(z)$, however, the model is not identifiable and recovering components with maximal explained variance may not correspond to recovering the z_j 's.

Throughout, we additionally assume the following.²

Assumption 3.3 (IID noise). The exogenous noise variables are jointly independent and identically distributed. That is, $u_1, \dots, u_d \stackrel{\text{iid}}{\sim} \rho$ for some probability measure ρ .

Thm. 3.3 rules out hidden confounding and guarantees that the induced distribution is Markov w.r.t. the induced causal graph \mathcal{G} , i.e., that it obeys the following factorization,

$$p_{\mathcal{M}}(\mathbf{z}) = \prod_{j=1}^d p_{\mathcal{M}}(z_j | \mathbf{z}_{\text{pa}(j)}). \quad (3.3)$$

The structural assignments in Eq. (3.2) represent independent mechanisms which remain invariant if other parts of the model change. Interventions are modelled by replacing a subset of these mechanisms in the original model. Here, we consider interventions (deterministic or stochastic, perfect or imperfect) which do not introduce new parents.

Definition 3.4 (Interventions). An *intervention* on targets $\mathcal{I} \subseteq [d]$ in an acyclic SCM $\mathcal{M} = (\mathbf{F}, \rho)$ replaces a subset of assignments in \mathbf{F} with new assignments

$$\{z_j := h_j(\mathbf{z}_{\text{pa}(j)}, \tilde{u}_j)\}_{j \in \mathcal{I}}$$

such that Thm. 3.3 holds for the new noise variables $\tilde{\mathbf{u}}_{\mathcal{I}} \cup \mathbf{u}_{[d] \setminus \mathcal{I}}$. This yields a modified SCM $\mathcal{M}' = (\mathbf{F}', \rho)$, where \mathbf{F}' matches \mathbf{F} except that f_j is replaced by h_j for all $j \in \mathcal{I}$. The resulting *interventional distribution* and *post-intervention graph* \mathcal{G}' are those induced by \mathcal{M}' .

We now specify the true prior structure by linking the observed action labels to interventions in an unknown underlying SCM. Specifically, we consider the case of binary $\mathbf{a}_e \in \{0, 1\}^{d_Z}$ indicating the intervention targets in domain e , see § 8 for a discussion of alternative choices.

Assumption 3.5 (Interventional priors with known targets and causal graph). There exists an acyclic SCM \mathcal{M}^* over \mathbf{z} satisfying Thm. 3.3 such that for all $e \in [M]$ the true prior $p^*(z | \mathbf{a}_e)$ is an interventional distribution induced by an intervention on targets $\mathcal{I}(\mathbf{a}_e) = \{j \mid a_{ej} = 1\}$ in \mathcal{M}^* and

$$(\mathbf{z}_{ei})_{i \in [N_e]} \stackrel{\text{iid}}{\sim} p^*(z | \mathbf{a}_e).$$

Moreover, the causal graph \mathcal{G}^* induced by \mathcal{M}^* is known.

Under Thm. 3.5, for all $e \in [M]$, $i \in [N_e]$, and $j \in [d_Z]$, the mechanism that gives rise to z_{eij} is given by

$$z_{eij} := \begin{cases} f_j(\mathbf{z}_{ei\text{pa}(j)}, u_{eij}), & \text{if } a_{ej} = 0, \\ h_j(\mathbf{z}_{ei\text{pa}(j)}, \tilde{u}_{eij}), & \text{if } a_{ej} = 1, \end{cases} \quad (3.4)$$

²Thm. 3.3 is slightly stronger than causal sufficiency, which only implies independence of the noise variables. Here, we also assume identical marginal distributions for convenience.

where f_j is the baseline and h_j the interventional mechanism when node j is targeted by \mathbf{a}_e . This extends the classical empirical Bayes, which would assume $z_{eij} \stackrel{\text{iid}}{\sim} g$ for a single, shared, learnable prior g [15, 21].

4 ESTIMATION AND INFERENCE

Causal representation learning (CRL) is naturally a simultaneous inference problem, as its goal is to recover the causal variables $\{z_{ei}\}_{i \in [N_e], e \in [M]}$ from the available multi-domain data \mathcal{D} in Eq. (2.1). This amounts to $\sum_{e=1}^M N_e$ simultaneous inference problems of computing the posteriors $p^*(z_{ei} | \mathbf{x}_{ei}, \mathbf{a}_e)$ in Eq. (2.3), thus creating an opportunity to apply the empirical Bayes (EB) methodology.

The main challenge for posterior inference is that the measurement model parameters \mathbf{A}^* and σ^{2*} and the priors $p^*(z | \mathbf{a}_e)$ are unknown.³ EB methods infer these quantities via Thm. 2.1 and fall into two categories, g-modeling and f -modeling, depending on how they handle the prior [21].

In g-modeling, the prior (typically denoted g) is modeled explicitly and estimated jointly with the other unknowns by approximately optimizing the marginal likelihood of \mathcal{D} . The fitted model is then used for posterior inference.

In f -modeling, the learning of the prior remains implicit. Instead, posterior quantities are estimated directly by modeling the marginal density (typically denoted f) of the observed data [13]. This is often done via the classical Robbins-Tweedie formula, which uses the score of the marginal likelihood to approximate the posterior mean and covariance of the local latent variables [11, 12, 28].

In the present work, we focus on f -modeling via Tweedie’s formula and adapt this method to our multi-domain CRL setting. As we will show, f -modeling provides a direct route to obtaining the posterior summaries of $p^*(z | \mathbf{x}, \mathbf{a})$ by estimating the data distribution $p^*(\mathbf{x} | \mathbf{a})$ in Eq. (2.2), without ever explicitly learning the domain-specific priors $p^*(z | \mathbf{a}_e)$. Specifically, we develop an expectation maximization (EM) [9] algorithm for CRL f -modeling, which leverages a causally-structured score estimator. In the remainder of this section, we describe the main steps of this algorithm. Details on score estimation are deferred to § 5.

4.1 HIGH-LEVEL EM PROCEDURE

Our EM f -modeling algorithm for model (3.1) iterates between estimating the first and second moments of the latent causal variables z_{ei} (E-step) and estimating the measurement model parameters, i.e., the mixing matrix \mathbf{A} and the

³According to Thm. 3.5 the causal graph underlying $p^*(z | \mathbf{a})$ is known and the intervention targets in domain e are given by \mathbf{a}_e . However, the shared base causal mechanisms $\{f_j\}_{j \in [d_Z]}$ and the intervened mechanisms $\{h_j\}_{j \in [d_Z]}$ in Eq. (3.4) are unknown.

Algorithm 1 EM f -modeling with causal score matching

Require: Data $\mathcal{D} = \{((\mathbf{x}_{ei})_{i=1}^{N_e}, \mathbf{a}_e)\}_{e=1}^M$, causal graph $\mathcal{G} = ([d_Z], \mathcal{E})$, iterations T , damping factor $\eta \in (0, 1)$. Initialize $\hat{\mathbf{A}} = \hat{\mathbf{O}}\hat{\mathbf{D}}$ with $\hat{\mathbf{O}} \in \mathcal{O}^{d_X \times d_Z}$ and $\hat{\mathbf{D}} \in \mathbb{R}^{d_Z \times d_Z}$ diagonal, score components $\{\hat{\sigma}_j\}_{j \in [d_Z]}$, and $\hat{\sigma}^2 > 0$.
for $t = 1$ **to** T **do**
 Compute $\mathbf{y}_{ei} \leftarrow \hat{\mathbf{O}}^\top \mathbf{x}_{ei}$ for all $e \in [M]$ and $i \in [N_e]$.
 Update $\hat{\sigma}$ via causal score matching: (5.4) and (5.5).
 Update \hat{z}_{ei} and \hat{z}_{ei}^2 using the first- and second-order Tweedie formulas in (4.4) and (4.5).
 Update $\hat{\mathbf{A}} = \hat{\mathbf{O}}\hat{\mathbf{D}}$ via the analytical steps in (4.8).
 Update $\hat{\sigma}^2$ using the MLE in (4.9).
end for
return $\{\hat{z}_{ei}\}_{e \in [M], i \in [N_e]}, \hat{\mathbf{A}}, \hat{\sigma}^2$.

noise variance σ^2 (M-step). Each iteration runs in two steps:

- E:** Fix the current estimate $\hat{\mathbf{A}}$ and $\hat{\sigma}^2$ and compute the posterior mean \hat{z}_{ei} and element-wise second moments \hat{z}_{ei}^2 using Tweedie’s formula [11], combined with score matching [18] (see § 5 for details on score estimation).
- M:** Update $\hat{\mathbf{A}}$ and $\hat{\sigma}^2$ by (approximately) maximizing the likelihood given the current posterior summaries \hat{z}_{ei} and \hat{z}_{ei}^2 from the E-step.

The full procedure, which alternates these updates for a fixed number of iterations, is summarized in Alg. 1. We will also refer to the algorithm as *CRL f -modeling*. Whereas the M-step is relatively straight-forward, the E-step is more involved; this is also where our causal assumptions enter.

4.2 TWEEDIE’S FORMULA

The focal point of traditional empirical Bayes theory is the normal means model with isotropic noise [13–15, 38, 42],

$$\mathbf{x}_i = \boldsymbol{\theta}_i + \boldsymbol{\zeta}_i, \quad \boldsymbol{\zeta}_i \stackrel{\text{iid}}{\sim} \mathcal{N}(\mathbf{0}, \sigma^2 \mathbf{I}_{d_X}). \quad (4.1)$$

A central result is Tweedie’s formula [21, Thm. 6.2], which states that the optimal estimator t^* minimizing the posterior risk $\mathbb{E}[\|\boldsymbol{\theta} - t(\mathbf{x}_i)\|_2^2]$ for any prior on $\boldsymbol{\theta}_i$ is given by

$$t^*(\mathbf{x}_i) := \mathbb{E}[\boldsymbol{\theta}_i | \mathbf{x}_i] = \mathbf{x}_i + \sigma^2 \nabla \log f(\mathbf{x}_i),$$

where f denotes the marginal density of \mathbf{x} .

By applying Tweedie’s formula to model (3.1), we can recover the posterior mean of $\mathbf{A}\mathbf{z}$ given \mathbf{x} . However, this does not lead to the posterior mean of \mathbf{z} as \mathbf{A} need not be invertible. To solve this problem, we impose an additional assumption on the class of mixing matrices \mathbf{A} that allows us to reduce the problem to a normal means model.

4.3 REDUCTION TO NORMAL MEANS MODEL

To model the causal variable \mathbf{z} via Tweedie’s formula, we impose the following orthogonality assumption on \mathbf{A}^* .

Assumption 4.1. The true mixing matrix \mathbf{A}^* satisfies $(\mathbf{A}^*)^\top \mathbf{A}^* = (\mathbf{D}^*)^2$ for some diagonal $\mathbf{D}^* \in \mathbb{R}^{d_z \times d_z}$.

Thm. 4.1 states that the columns of \mathbf{A}^* are orthogonal with possibly different norms, similar to assumptions exploited in independent mechanism analysis [17, 36] or principal component flows [8]. Thm. 4.1 allows us to parametrize \mathbf{A} as $\mathbf{A} := \mathbf{O}\mathbf{D}$, where $\mathbf{O} \in \mathcal{O}^{d_x \times d_z}$ is orthonormal and $\mathbf{D} \in \mathbb{R}^{d_z \times d_z}$ is diagonal.

Let $\mathbf{y}_{ei} := \mathbf{O}^\top \mathbf{x}_{ei}$. Since $\mathbf{O}^\top \mathbf{O} = \mathbf{I}_{d_z}$, multiplying both sides of the linear measurement model in (3.1) by \mathbf{O}^\top then yields the following (multi-domain) normal means model,

$$\mathbf{y}_{ei} = \mathbf{D}\mathbf{z}_{ei} + \zeta_{ei}, \quad \zeta_{ei} \stackrel{\text{iid}}{\sim} \mathcal{N}(0, \sigma^2 \mathbf{I}_{d_z}). \quad (4.2)$$

4.4 UPDATING THE LATENT VARIABLES

According to Tweedie’s formula applied to Eq. (4.2), the optimal estimator for the means $\mathbf{D}\mathbf{z}_{ei}$ is given by

$$\mathbb{E}[\mathbf{D}\mathbf{z}_{ei} | \mathbf{y}_{ei}] = \mathbf{y}_{ei} + \sigma^2 \nabla \log f_{\mathbf{a}_e}(\mathbf{y}_{ei}), \quad (4.3)$$

where $f_{\mathbf{a}_e}$ is the true marginal density of \mathbf{y} in domain e , defined as the push-forward of $p^*(\mathbf{z} | \mathbf{a}_e)$ via (4.2).

For fixed $\hat{\mathbf{A}} = \hat{\mathbf{O}}\hat{\mathbf{D}}$ and $\hat{\sigma}^2$, we therefore only need estimates of the scores $\nabla \log f_{\mathbf{a}_e}(\mathbf{y}_{ei})$ to estimate the posterior mean of \mathbf{z}_{ei} via (4.3). In § 5, we discuss how we estimate these scores using a flexible function class to obtain an estimate $\hat{\mathbf{s}}(\mathbf{y}, \mathbf{a})$ via score matching [18]. We then update the empirical Bayes estimates of all local latent variables \mathbf{z}_{ei} using a damped version of Tweedie’s formula:

$$\widehat{\mathbf{z}}_{ei} = \hat{\mathbf{D}}^{-1} \left(\mathbf{y}_{ei} + \eta \hat{\sigma}^2 \hat{\mathbf{s}}(\mathbf{y}_{ei}, \mathbf{a}_e) \right), \quad (4.4)$$

where $\eta \in [0, 1]$ is the damping factor; $\eta = 0$ corresponds to no shrinkage and $\eta = 1$ to the classical Tweedie’s formula.

We also require the posterior second moments, defined as the element-wise squares $\mathbb{E}[\mathbf{z}_{ei} \odot \mathbf{z}_{ei} | \mathbf{x}_{ei}, \mathbf{a}_e]$. To approximate them, we use the following estimates $\widehat{\mathbf{z}}_{ei}^2 \in \mathbb{R}^{d_z}$ obtained from the second-order Tweedie formula [12, 43]:

$$\widehat{\mathbf{z}}_{ei}^2 = \widehat{\mathbf{z}}_{ei}^2 + \hat{\sigma}^2 \hat{\mathbf{D}}^{-2} + \hat{\sigma}^4 \hat{\mathbf{D}}^{-2} \partial_j \hat{\mathbf{s}}_j(\mathbf{y}_j, \mathbf{y}_{\text{pa}(j)}, \mathbf{a}_e), \quad (4.5)$$

where the component-wise score estimates $\hat{\mathbf{s}}_{jj}$ for $j \in [d_z]$ are described in further detail in § 5.

4.5 UPDATING THE MEASUREMENT MODEL

Given our estimates of the posterior first and second moments of each \mathbf{z}_{ei} , in the M-step we update the parameters

(\mathbf{A}, σ^2) to maximize the data log-likelihood, resulting in

$$\hat{\mathbf{A}}, \hat{\sigma}^2 \in \arg \max_{\mathbf{A}=\mathbf{O}\mathbf{D}, \sigma^2 \geq 0} \sum_{e=1}^M \sum_{i=1}^{N_e} \mathbb{E}_{\widehat{\mathbf{q}}_{ei}(\mathbf{z})} \left[\log p_{\mathbf{A}, \sigma^2}(\mathbf{x}_{ei} | \mathbf{z}) \right], \quad (4.6)$$

where $\widehat{\mathbf{q}}_{ei}$ is the posterior distribution that we approximated via (4.4) and (4.5) in the E-step. The M-step objective also corresponds to the first (energy) term in the ELBO, see § 6.

Since $\log p_{\mathbf{A}, \sigma^2}(\mathbf{x}_{ei} | \mathbf{z}_{ei})$ is quadratic in \mathbf{z}_{ei} under the Gaussian measurement model (Thm. 3.1), this objective depends on $\widehat{\mathbf{q}}_{ei}$ only through its first and second moments. Thus, we replace $\mathbb{E}_{\widehat{\mathbf{q}}_{ei}}[\mathbf{z}_{ei}]$ and $\mathbb{E}_{\widehat{\mathbf{q}}_{ei}}[\mathbf{z}_{ei} \odot \mathbf{z}_{ei}]$ by the empirical Bayes estimates $\widehat{\mathbf{z}}_{ei}$ and $\widehat{\mathbf{z}}_{ei}^2$ to obtain objectives for \mathbf{A} and σ^2 , see § A for the detailed derivations.

Updating $\hat{\mathbf{A}}$. Given the estimates $\widehat{\mathbf{z}}_{ei}$ and $\widehat{\mathbf{z}}_{ei}^2$, we learn \mathbf{A} by the maximum likelihood estimator (MLE),

$$\hat{\mathbf{A}} \in \arg \min_{\mathbf{A}=\mathbf{O}\mathbf{D}} \sum_{e=1}^M \sum_{i=1}^{N_e} \left[\sum_{j=1}^{d_z} \mathbf{D}_{jj}^2 \widehat{\mathbf{z}}_{ej}^2 - 2\mathbf{x}_{ei}^\top \mathbf{A} \widehat{\mathbf{z}}_{ei} \right]. \quad (4.7)$$

The solution $\hat{\mathbf{A}} = \hat{\mathbf{O}}\hat{\mathbf{D}}$ to (4.7) can be computed analytically in the following steps:

$$\begin{aligned} \mathbf{M} &\leftarrow \sum_{e=1}^M \sum_{i=1}^{N_e} \mathbf{x}_{ei} \widehat{\mathbf{z}}_{ei}^\top, & [\mathbf{U}, \mathbf{\Sigma}, \mathbf{V}] &\leftarrow \text{SVD}(\mathbf{M}), \\ \hat{\mathbf{O}} &\leftarrow \mathbf{U}\mathbf{V}^\top, & \hat{\mathbf{D}}_{jj}^2 &\leftarrow \frac{\mathbf{\Sigma}_{jj}}{\sum_{e=1}^M \sum_{i=1}^{N_e} \widehat{\mathbf{z}}_{ej}^2}, \end{aligned} \quad (4.8)$$

Updating $\hat{\sigma}^2$. Finally, we update σ^2 with the MLE:

$$\hat{\sigma}^2 = \frac{\sum_{e=1}^M \sum_{i=1}^{N_e} \left[\sum_{j=1}^{d_z} \hat{\mathbf{D}}_{jj}^2 \widehat{\mathbf{z}}_{ej}^2 - 2\mathbf{x}_{ei}^\top \hat{\mathbf{A}} \widehat{\mathbf{z}}_{ei} + \|\mathbf{x}_{ei}\|^2 \right]}{d_X \sum_{e=1}^M N_e}. \quad (4.9)$$

Together, Eq. (4.4)–(4.5) form the E-steps and Eq. (4.7)–(4.9) form the M-steps of the EM algorithm. The full algorithm iterates between the E- and M-steps until convergence.

4.6 RELAXING ORTHOGONALITY

Thm. 4.1 can be relaxed to $(\mathbf{A}^*)^\top \mathbf{A}^* = (\mathbf{\Lambda}^*)^2$ for an unknown positive semi-definite (p.s.d.) matrix $\mathbf{\Lambda}^*$. This is equivalent to assuming that $\mathbf{A}^* = \mathbf{O}^* \mathbf{\Lambda}^*$ for some orthonormal matrix \mathbf{O}^* . Accordingly, we parametrize $\mathbf{A} = \mathbf{O}\mathbf{\Lambda}$ with $\mathbf{O} \in \mathcal{O}^{d_x \times d_z}$ and $\mathbf{\Lambda}$ a p.s.d. matrix. The only modifications needed are to replace \mathbf{D}^{-1} with $\mathbf{\Lambda}^{-1}$ in Tweedie’s update in (4.4) and replace the steps in (4.8) with updates for \mathbf{O} and $\mathbf{\Lambda}$ that solve Eq. (4.7). The second-order Tweedie update from (4.5) also generalizes: with $\mathbf{J}_{\hat{\mathbf{s}}}(\mathbf{y}_{ei}, \mathbf{a}_e)$ denoting the Jacobian of $\hat{\mathbf{s}}(\cdot, \mathbf{a}_e)$ evaluated at \mathbf{y}_{ei} , we obtain [28, Thm. 1]:

$$\widehat{\mathbf{z}}_{ei}^2 = \widehat{\mathbf{z}}_{ei}^2 + \left[\hat{\sigma}^2 \hat{\mathbf{\Lambda}}^{-2} + \hat{\sigma}^4 \hat{\mathbf{\Lambda}}^{-1} \mathbf{J}_{\hat{\mathbf{s}}}(\mathbf{y}_{ei}, \mathbf{a}_e) \hat{\mathbf{\Lambda}}^{-1} \right]_{jj}.$$

5 CAUSAL SCORE MATCHING

Approximating the posterior of \mathbf{z} via Tweedie’s formula in Eqs. (4.3) to (4.5) involves the score function $\nabla \log f_{\mathbf{a}}(\mathbf{y})$. In this section, we propose a scalable method to estimate this score that allows for incorporating knowledge of the causal directed acyclic graph (DAG) \mathcal{G}^* from Thm. 3.5.

Score decomposition. The true marginal $f_{\mathbf{a}_e}(\mathbf{y}_{ei})$ is determined by the normal means model in (4.2) and depends on \mathbf{a}_e only through $\mathbf{z}_{ei} \sim p^*(\mathbf{z} | \mathbf{a}_e)$. Under Thm. 3.5, the score of \mathbf{z} follows from the Markov factorization in Eq. (3.3) w.r.t. the true causal graph \mathcal{G}^* . Its j^{th} component is given by

$$\begin{aligned} [\nabla \log p^*(\mathbf{z} | \mathbf{a})]_j &= \partial_j \log p^*(z_j | \mathbf{z}_{\text{pa}(j)}, a_j) \\ &+ \sum_{k \in \text{ch}(j)} \partial_j \log p^*(z_k | \mathbf{z}_{\text{pa}(k)}, a_k) \end{aligned} \quad (5.1)$$

and only depends on the Markov blanket [30] of z_j and the intervention target labels for z_j and its children.⁴

Even though \mathbf{y} is simply a noisy, element-wise rescaling of \mathbf{z} , the decomposition from Eq. (5.1) need not hold for the score $\nabla \log f_{\mathbf{a}}(\mathbf{y})$ due to the additional noise term ζ in Eq. (4.2). Instead, the factorization of $f_{\mathbf{a}}(\mathbf{y})$ is determined by d-separation [31] in the extended graph of \mathcal{G}^* with additional nodes for \mathbf{y} and \mathbf{a} and additional edges $\{a_j \rightarrow z_j \rightarrow y_j\}_{j \in [d_Z]}$, see Fig. 2 for an example.

In general, each component of $\nabla \log f_{\mathbf{a}}(\mathbf{y})$ may depend on most or all of \mathbf{y} and \mathbf{a} , i.e., it is a dense vector field [4, §13.1]. This poses challenges for estimation, particularly when d_Z is large. We therefore propose a sparse approximation of the true score that incorporates prior causal knowledge.

Causal score function. Specifically, we consider the class of *causal score functions* $s : \mathbb{R}^{d_Z} \times \{0, 1\}^{d_Z} \rightarrow \mathbb{R}^{d_Z}$ w.r.t. a given DAG \mathcal{G} over $[d_Z]$, defined component-wise by

$$[s(\mathbf{y}, \mathbf{a})]_j := s_j(y_j, \mathbf{y}_{\text{pa}(j; \mathcal{G})}, a_j), \quad (5.2)$$

where $\text{pa}(j; \mathcal{G})$ refers to the parents in \mathcal{G} . Natural choices of \mathcal{G} include $\mathcal{G} = \mathcal{G}^*$, the empty graph, and complete DAGs w.r.t. the partial causal ordering induced by \mathcal{G}^* .⁵

We fit the causal score function s via score-matching [18] w.r.t. the true score, which on the population level is equivalent to minimizing the following L_2 loss,

$$L^{\mathcal{G}}(s) = \sum_{e=1}^M \mathbb{E}_{\mathbf{y} \sim f_{\mathbf{a}_e}} \left[\left\| s(\mathbf{y}, \mathbf{a}_e) - \nabla \log f_{\mathbf{a}_e}(\mathbf{y}) \right\|_2^2 \right]. \quad (5.3)$$

⁴The Markov blanket of node j in a DAG comprises j , the parents and children of j , and all other parents of children of j .

⁵Using a sparser DAG can be beneficial from a bias-variance perspective: while the restricted class (5.2) may be biased for the full score, restricting inputs to $\text{pa}(j)$ can reduce the variance of score estimation relative to conditioning on a larger set. It also reduces computational cost and thus scales better to large DAGs.

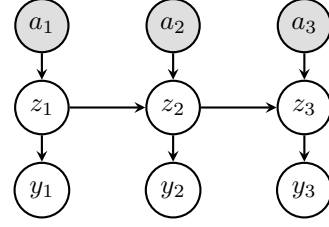


Figure 2: **Example DAG with intervention targets and surrogate latents.** The chain graph over \mathbf{z} implies $z_1 \perp\!\!\!\perp z_3 | z_2$ and $z_j \perp\!\!\!\perp a_k | z_{j-1}$ for $k \neq j$. Yet, due to measurement error, $y_1 \not\perp\!\!\!\perp y_3 | y_2$ and $y_j \not\perp\!\!\!\perp a_l | \mathbf{y}_{-j}$ for $l \leq k$. This illustrates why $\nabla \log f_{\mathbf{a}}(\mathbf{y})$ is generally dense.

The optimal causal score function s^* minimizing Eq. (5.3) coincides with $\nabla \log f_{\mathbf{a}}(\mathbf{y})$ (i.e., the approximation is exact) when $\mathcal{G} = \mathcal{G}^*$ is the empty graph. Similarly, when $\mathcal{G} = \mathcal{G}^*$ and $\sigma^2 = 0$ (and thus $\mathbf{y} = \mathbf{D}\mathbf{z}$), the optimal causal score recovers the true score for leaf nodes j (for which $\text{ch}(j) = \emptyset$ and the second term on the RHS of Eq. (5.1) vanishes). Otherwise, it serves as a sparse, structured approximation.

Besides generally enforcing sparsity, the specific choice of arguments to s_j on the RHS of Eq. (5.2) is informed by adherence to the causal generative process. Under the assumed interventional SCM priors (Thm. 3.5), each latent z_j depends only on $\mathbf{z}_{\text{pa}(j)}$ and a_j . However, this factorization generally need not hold for the marginal distribution of the Tweedie estimates $\{\hat{z}_{ei}\}_{i \in [N_e]}$ from (4.4) as $N_e \rightarrow \infty$, even in the noiseless case, since (5.1) also includes contributions from children, their intervention targets, and other parents.

If we view y_j as a noisy surrogate of z_j , it therefore seems natural to posit that the estimator \hat{z}_j derived from (4.3) should depend only on $(y_j, \mathbf{y}_{\text{pa}(j; \mathcal{G})}, a_j)$. If $\mathcal{G} = \mathcal{G}^*$, this restriction guarantees that, as $N_e \rightarrow \infty$, the empirical distribution $\frac{1}{N_e} \sum_{i=1}^{N_e} \delta_{\hat{z}_{ei}}$ of the Tweedie estimates $\{\hat{z}_{eij}\}_{i \in [N_e]}$ in Eq. (4.4) depends only on $(z_j, \mathbf{z}_{\text{pa}(j)}, a_j)$. Moreover, the approximation $[s(\cdot, \mathbf{a})]_j = s_j(\cdot, a_j)$ becomes accurate in the large-sample regime, as discussed in § A.3.

Decoupled estimation. The following result characterizes the structure for the minimizer of the score-matching loss.

Theorem 5.1. *For all solutions $s^* \in \arg \min_{s \in \mathcal{S}} L^{\mathcal{G}}(s)$ and all $j \in [d_Z]$, the j^{th} component s_j^* of s^* minimizes*

$$\sum_{e=1}^M \mathbb{E}_{\mathbf{y} \sim f_{\mathbf{a}_e}} \left[\left| s_j(y_j, \mathbf{y}_{\text{pa}(j)}, a_{ej}) \right|^2 + 2\partial_j s_j(y_j, \mathbf{y}_{\text{pa}(j)}, a_{ej}) \right]. \quad (5.4)$$

Thm. 5.1 provides a key structural insight into the causal score-matching problem: The optimization over s decouples across the components $\{s_j\}_{j=1}^{d_Z}$. To learn the causal score, it thus suffices to solve d_Z smaller score-matching problems.

Empirical considerations. In practice, we only have the finite sample from (2.1) and do not know \mathbf{A} (nor \mathbf{y}). At each iteration of Alg. 1, we therefore use the current estimate $\widehat{\mathbf{A}} = \widehat{\mathbf{O}}\widehat{\mathbf{D}}$ of \mathbf{A} to form the pseudo-latents $\mathbf{y}_{ei} = \widehat{\mathbf{O}}^\top \mathbf{x}_{ei}$ and estimate each \widehat{s}_j by minimizing the empirical version $\widehat{\mathcal{L}}_j^{\mathcal{G}}$ of the loss in Eq. (5.4) obtained by replacing the expectation by an empirical average over $\{\mathbf{y}_{ei}\}_{i=1}^{N_e}$:

$$\widehat{s}_j \in \arg \min_{s_j} \widehat{\mathcal{L}}_j^{\mathcal{G}}(s_j). \quad (5.5)$$

Once we obtain the estimates $\{\widehat{s}_j\}_{j \in [d_Z]}$, the full score estimate $\widehat{\mathbf{s}}$ is a d_Z -dimensional vector field such that

$$[\widehat{\mathbf{s}}(\mathbf{y}, \mathbf{a})]_j = \widehat{s}_j(\mathbf{y}_j, \mathbf{y}_{\text{pa}(j)}, \mathbf{a}_j).$$

Estimation with cubic splines. In practice, each score component s_j is parameterized by a nonparametric function class [47]. An example is the family of cubic splines, which yields a simple closed-form solution (see § A.1). The partial derivatives are computed efficiently, either in closed form or via automatic differentiation.

6 g-MODELING AND RELATED WORK

While our main focus is on the f -modeling approach developed in §§ 4 and 5, we now sketch g -modeling for our setting and use this perspective to discuss prior works, many of which (implicitly) fall into this category.

As discussed in § 4, g -modeling explicitly models the priors $p^*(\mathbf{z} \mid \mathbf{a}_e)$ via a parametric family $\{p_\gamma(\mathbf{z} \mid \mathbf{a}_e) : \gamma \in \Gamma\}$ and aims to jointly infer the parameters $\boldsymbol{\theta} := (\mathbf{A}, \sigma^2, \gamma)$ by maximizing the log marginal likelihood

$$\log p_\theta(\mathcal{D}) = \sum_{e=1}^M \sum_{i=1}^{N_e} \log p_\theta(\mathbf{x}_{ei} \mid \mathbf{a}_e), \quad (6.1)$$

$$\text{where } p_\theta(\mathbf{x} \mid \mathbf{a}) = \int p_{\mathbf{A}, \sigma^2}(\mathbf{x} \mid \mathbf{z}) p_\gamma(\mathbf{z} \mid \mathbf{a}) d\mathbf{z}.$$

Eq. (6.1) is difficult to optimize exactly because it involves intractable integrals. However, we can use variational inference (VI) to approximate it [5]. For any variational posterior $q_{ei} \in \mathcal{P}(\mathbb{R}^{d_Z})$ over \mathbf{z}_{ei} , we can bound the marginal likelihood by the *evidence lower bound* (ELBO),

$$\log p_\theta(\mathbf{x}_{ei} \mid \mathbf{a}_e) \geq \text{ELBO}(\boldsymbol{\theta}, q_{ei}; \mathbf{x}_{ei}, \mathbf{a}_e) := \mathbb{E}_{q_{ei}(\mathbf{z})} [\log p_{\mathbf{A}, \sigma^2}(\mathbf{x}_{ei} \mid \mathbf{z})] - D_{\text{KL}}(q_{ei}(\mathbf{z}) \parallel p_\gamma(\mathbf{z} \mid \mathbf{a}_e)).$$

The variational posteriors often come from a parametric family $\{q_\phi(\mathbf{z}) : \phi \in \Phi\}$. Provided p_γ is differentiable w.r.t. γ , black-box VI [35] or amortized VI with reparametrization trick [25, 37] yield differentiable objectives amenable to gradient-based optimization w.r.t. both $\boldsymbol{\theta}$ and ϕ . The learned variational posterior is then used as approximation of (2.3).

For a single domain and a parameter-free standard Gaussian prior, $p_\gamma(\mathbf{z}) = \mathcal{N}(\mathbf{0}, \mathbf{I})$, the above reduces to a vanilla (linear) VAE [25] or probabilistic PCA [45]. More expressive choices for $p_\gamma(\mathbf{z})$ include, e.g., a mixture of Gaussians [10], whose parameters γ are learned jointly with the measurement (\mathbf{A}, σ^2) and variational ϕ parameters, in the spirit of g -modeling. Alternatively, the prior can be expressed directly in terms of the variational posterior [46], which leverages the fixed-point identity for $p^*(\mathbf{z} \mid \mathbf{a})$ implied by Thm. 2.1.

If we observe multiple domains and do not impose additional structure on $p_\gamma(\mathbf{z} \mid \mathbf{a})$, we obtain a conditional VAE [41]. The iVAE [24] is a conditional VAE in which $p_\gamma(\mathbf{z} \mid \mathbf{a})$ is factorized and from an exponential family whose natural parameters depend on \mathbf{a} . It is identifiable if the set of observed domains \mathcal{A} is sufficiently diverse. For single-cell data, perturbations \mathbf{a}_e are commonly modeled at the level of $p_\gamma(\mathbf{z} \mid \mathbf{a}_e)$ as additive mean shifts [3, 27, 52].

To parametrize the interventional prior from Thm. 3.5, let

$$z_{eij} = \gamma_j(\mathbf{a}_{ej}, \mathbf{z}_{eip\mathbf{a}(j)}, u_{eij}), \quad u_{eij} \stackrel{\text{iid}}{\sim} \text{UNIF}[0, 1], \quad (6.2)$$

where each γ_j is a nonlinear function that models the causal mechanism from (3.4) as $\gamma_j(0, \cdot, \cdot) = f_j(\cdot, \cdot)$ and $\gamma_j(1, \cdot, \cdot) = h_j(\cdot, \cdot)$. Several CRL methods amount to some form of g -modeling with a prior as in (6.2) [6, 51, 56, 58].

7 EMPIRICAL STUDIES

Our empirical studies evaluate the performance of CRL f -modeling, where the aim is to recover the causal variables and the mixing matrix from multiple interventional datasets with known causal graph and intervention targets.

Data. We generate synthetic data from an SCM over $d_Z = 4$ latent variables arranged in a chain $z_1 \rightarrow z_2 \rightarrow z_3 \rightarrow z_4$. For each node $j \in [d_Z]$, the structural equation is

$$z_j := \sum_{k \in \text{pa}(j)} w_{jk} g(z_k) + u_j, \quad (7.1)$$

with $w_{jk} \stackrel{\text{iid}}{\sim} \text{UNIF}[-1, 1]$, noise $u_j \stackrel{\text{iid}}{\sim} \mathcal{N}(0, \sigma_z^2)$ with $\sigma_z^2 = 4$, and nonlinearity $g(z) = \tanh(\kappa z) + (\kappa z)^3$ with $\kappa = 3$. Each domain results from a single-node intervention with targets encoded by a one-hot vector $\mathbf{a} \in \{0, 1\}^{d_Z}$ such that an intervention on z_j replaces the corresponding structural equation from (7.1) with $z_j := \tilde{u}_j \sim \mathcal{N}(10, 1)$. The latents $\mathbf{z} \in \mathbb{R}^{d_Z}$ are mapped to observations $\mathbf{x} \in \mathbb{R}^{d_X}$ with $d_X = 100$ via the linear measurement model from (3.1), where $\mathbf{A}^* \in \mathcal{O}^{d_X \times d_Z}$ is a random column-orthonormal matrix and $\sigma^{2*} = 2$.

Baselines. We compare the proposed CRL f -modeling approach with versions thereof which use no shrinkage (i.e., $\eta = 0$ in Tweedie’s formula) or which incorrectly assume an empty or complete (w.r.t. the true causal order) causal graph.

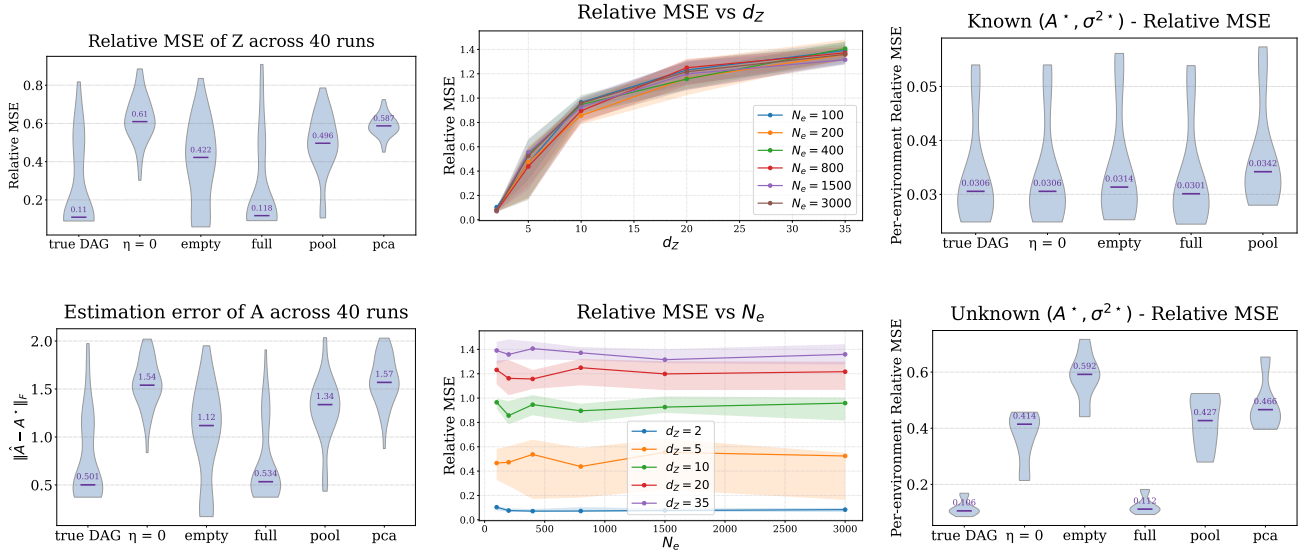


Figure 3: **Empirical performance of CRL f -modeling.** (Left column:) relative MSE (top) and Frobenius error of $\hat{\mathbf{A}}$ (bottom). (Middle column:) scaling of relative MSE with d_Z (top) and with N_e (bottom) across 20 runs, with $d_X = 100$. Solid curves show the median across runs and shaded bands show the interquartile range. (Right column:) per-environment relative MSE in the oracle setting (top; known \mathbf{A}^* , σ^{2*}) and in the learned setting (bottom; unknown \mathbf{A}^* , σ^{2*}).

We also consider baselines that ignore the interventional multi-domain structure (i.e., setting $\mathbf{a}_e = \mathbf{0}$ for all e) and apply either CRL f -modeling or PCA on the pooled data.

Metrics. We consider two metrics to assess estimation accuracy. The *relative MSE* (RelMSE) normalizes the squared estimation error by the norm of the true latent:

$$\text{RelMSE}(\hat{\mathbf{z}}, \mathbf{z}^*) := \frac{\|\hat{\mathbf{z}} - \mathbf{z}^*\|_2^2}{\|\mathbf{z}^*\|_2^2}. \quad (7.2)$$

In our analysis, we report RelMSE (7.2) averaged within a run, or within each environment.

The second metric we report is the Frobenius error of $\hat{\mathbf{A}}$:

$$\|\hat{\mathbf{A}} - \mathbf{A}^*\|_F^2 = \sum_{i=1}^{d_X} \sum_{j=1}^{d_Z} (\hat{\mathbf{A}}_{ij} - \mathbf{A}^*_{ij})^2. \quad (7.3)$$

Here $\hat{\mathbf{A}}$ is the final estimate of Alg. 1 after aligning the signs and permutation of its columns to best match \mathbf{A}^* . This follows from the identifiability results in § E that \mathbf{A}^* is identifiable up to signed permutations of its columns.

Code. A Python implementation of our CRL f -modeling algorithm (Alg. 1) and code to reproduce our results are available at: github.com/bohanwu2000/EB-CRL.

Results. The left column of Fig. 3 reports the two metrics across 40 runs. The main takeaways are as follows:

1. CRL f -modeling with the true DAG (TRUE DAG) and the complete DAG (FULL) outperform the other methods.

The latter performs well, presumably because it flexibly approximates the true score (see the discussion in § 5).

2. CRL f -modeling with an empty graph (EMPTY) is less stable across runs: misspecification leads to underperformance when effects of causal parents are strong.
3. CRL f -modeling on pooled data without intervention information (POOL) performs better than no shrinkage ($\eta = 0$) but worse than other EB methods.
4. As baselines, PCA on pooled data and Alg. 1 with no shrinkage ($\eta = 0$) perform worse than all EB methods.

The middle column of Fig. 3 reports the relative MSE of CRL f -modeling with the true DAG as d_Z and N_e vary. The relative MSE increases approximately like $O(\sqrt{d_Z})$ in d_Z and stabilizes once $N_e \geq 200$. The computational cost of CRL f -modeling with the true DAG scales like $O\left(\exp\left(\max_{j \in [d_Z]} |\text{pa}(j)|\right)\right)$, while CRL f -modeling with the complete DAG becomes challenging for large d_Z since it scales as $O(\exp(d_Z))$; see § A.1 for details.

The right column of Fig. 3 zooms in on per-environment performance by reporting results in both the oracle setting (where \mathbf{A}^* and σ^{2*} are known and held fixed) and the learned setting (where \mathbf{A} and σ^2 are learned). All empirical Bayes methods perform well in the oracle setting. In the learned setting, CRL f -modeling with the true DAG achieves the lowest error overall and remains relatively uniform across environments. Further details of the simulation study are relayed to § D.

8 DISCUSSION

We proposed an empirical Bayes f -modeling approach to multi-domain causal representation learning that addresses the simultaneous inference of latent causal variables under a noisy measurement model. The main EM algorithm performs iterative Tweedie updates with score matching. The empirical results show accurate performance.

When the true DAG is small or when the DAG is unknown but a causal order is known, it may be safer to run CRL f -modeling with the complete DAG induced by that order, since it is well specified for the true score function. When the DAG is large, CRL f -modeling with the true DAG is typically the more scalable and accurate choice.

For nonlinear measurement models, f -modeling is less directly applicable because of the difficulty to adapt Tweedie’s formula. On the other hand, g -modeling becomes more natural since it extends directly to nonlinear or learned decoders $p_{\theta}(x | z)$, including deep networks.

While our algorithm is rather focused on a particular scenario, we believe the framework of causal empirical Bayes to be more broadly applicable to other algorithms for other model classes. Extensions include richer intervention structures $p(z | a)$ with non-binary a (e.g., additive shifts) and relaxing the assumption of known graphs or targets by using the optimal EB objectives for graph/target discovery.

Acknowledgements

The authors thank Jonas Peters for insightful discussions during the conception of this work. JvK acknowledges support from The Branco Weiss Fellowship—Society in Science.

References

- [1] E. Acartürk, B. Varıcı, K. Shanmugam, A. Tajer, et al. Learning generative factors via causal representation learning: A score-based perspective. *IEEE BITS Information Theory Magazine*, 2026. [Cited on p. 1.]
- [2] K. Ahuja, D. Mahajan, Y. Wang, and Y. Bengio. Interventional causal representation learning. In *International Conference on Machine Learning*, pages 372–407. PMLR, 2023. [Cited on p. 1 and 16.]
- [3] M. Bereket and T. Karaletsos. Modelling cellular perturbations with the sparse additive mechanism shift variational autoencoder. In *Advances in Neural Information Processing Systems*, volume 36, pages 1–12, 2023. [Cited on p. 7.]
- [4] C. M. Bishop and N. M. Nasrabadi. *Pattern recognition and machine learning*, volume 4. Springer, 2006. [Cited on p. 6.]
- [5] D. M. Blei, A. Kucukelbir, and J. D. McAuliffe. Variational inference: A review for statisticians. *Journal of the American Statistical Association*, 112(518):859–877, 2017. [Cited on p. 7.]
- [6] J. Brehmer, P. De Haan, P. Lippe, and T. S. Cohen. Weakly supervised causal representation learning. In *Advances in Neural Information Processing Systems*, volume 35, pages 38319–38331, 2022. [Cited on p. 7.]
- [7] S. Buchholz, G. Rajendran, E. Rosenfeld, B. Aragam, B. Schölkopf, and P. Ravikumar. Learning linear causal representations from interventions under general nonlinear mixing. In *Advances in Neural Information Processing Systems*, volume 36, pages 45419–45462, 2023. [Cited on p. 1 and 16.]
- [8] E. Cunningham, A. D. Cobb, and S. Jha. Principal component flows. In *International Conference on Machine Learning*, pages 4492–4519. PMLR, 2022. [Cited on p. 5.]
- [9] A. P. Dempster, N. M. Laird, and D. B. Rubin. Maximum likelihood from incomplete data via the EM algorithm. *Journal of the Royal Statistical Society Series B: Statistical Methodology*, 39(1):1–22, 1977. [Cited on p. 4.]
- [10] N. Dilokthanakul, P. A. Mediano, M. Garnelo, M. C. Lee, H. Salimbeni, K. Arulkumaran, and M. Shanhahan. Deep unsupervised clustering with Gaussian mixture variational autoencoders. *arXiv preprint arXiv:1611.02648*, 2016. [Cited on p. 7.]
- [11] A. S. Eddington. The correction of statistics for accidental error. *Monthly Not. Roy. Astr. Soc.*, 100:354–361, 1940. [Cited on p. 4.]
- [12] B. Efron. Tweedie’s formula and selection bias. *Journal of the American Statistical Association*, 106, 2011. [Cited on p. 2, 4, and 5.]
- [13] B. Efron. Two modeling strategies for empirical Bayes estimation. *Statistical Science*, 29, 2014. [Cited on p. 4.]
- [14] B. Efron. Empirical Bayes deconvolution estimates. *Biometrika*, 103, 2015. [Cited on p. 2.]
- [15] B. Efron. Bayes, oracle Bayes and empirical Bayes. *Statistical Science*, 34(2):177–201, 2019. [Cited on p. 1 and 4.]
- [16] G. H. Golub and C. F. Van Loan. *Matrix Computations*. JHU press, 2013. [Cited on p. 13.]
- [17] L. Gresele, J. von Kügelgen, V. Stimper, B. Schölkopf, and M. Besserve. Independent mechanism analysis, a new concept? In *Advances in Neural Information Processing Systems*, volume 34, 2021. [Cited on p. 5.]

- [18] A. Hyvärinen and P. Dayan. Estimation of non-normalized statistical models by score matching. *Journal of Machine Learning Research*, 6(4), 2005. [Cited on p. 4, 5, 6, and 15.]
- [19] A. Hyvärinen and P. Pajunen. Nonlinear independent component analysis: Existence and uniqueness results. *Neural networks*, 12(3):429–439, 1999. [Cited on p. 1.]
- [20] A. Hyvärinen, H. Sasaki, and R. Turner. Nonlinear ica using auxiliary variables and generalized contrastive learning. In *The 22nd international conference on artificial intelligence and statistics*, pages 859–868. PMLR, 2019. [Cited on p. 1.]
- [21] N. Ignatiadis and B. Sen. *Empirical Bayes: From Herbert Robbins to Modern Theory and Applications*. 2025. [Cited on p. 1 and 4.]
- [22] W. James and C. Stein. Estimation with quadratic loss. In *Proceedings of the fourth Berkeley symposium on mathematical statistics and probability*, volume 1, pages 361–379. University of California Press, 1961. [Cited on p. 1.]
- [23] J. Jin and V. Syrgkanis. Learning linear causal representations from general environments: identifiability and intrinsic ambiguity. In *Advances in Neural Information Processing Systems*, volume 37, pages 63466–63509, 2024. [Cited on p. 1 and 16.]
- [24] I. Khemakhem, D. Kingma, R. Monti, and A. Hyvärinen. Variational autoencoders and nonlinear ICA: A unifying framework. In *International Conference on Artificial Intelligence and Statistics*, pages 2207–2217. PMLR, 2020. [Cited on p. 7.]
- [25] D. P. Kingma and M. Welling. Auto-encoding variational Bayes. In *International Conference on Learning Representations*, 2014. [Cited on p. 7.]
- [26] F. Locatello, S. Bauer, M. Lucic, G. Raetsch, S. Gelly, B. Schölkopf, and O. Bachem. Challenging common assumptions in the unsupervised learning of disentangled representations. In *International Conference on Machine Learning*, pages 4114–4124. PMLR, 2019. [Cited on p. 1.]
- [27] M. Lotfollahi, A. Klimovskaia Susmelj, C. De Donno, L. Hetzel, Y. Ji, I. L. Ibarra, S. R. Srivatsan, M. Naghipourfar, R. M. Daza, B. Martin, J. Shendure, J. L. McFaline-Figueroa, P. Boyeau, F. A. Wolf, N. Yakubova, S. Günemann, C. Trapnell, D. Lopez-Paz, and F. J. Theis. Predicting cellular responses to complex perturbations in high-throughput screens. *Molecular Systems Biology*, 19(6):e11517, 2023. [Cited on p. 7.]
- [28] C. Meng, Y. Song, W. Li, and S. Ermon. Estimating high order gradients of the data distribution by denoising. In *Advances in Neural Information Processing Systems*, volume 34, pages 25359–25369, 2021. [Cited on p. 4 and 5.]
- [29] G. Moran and B. Aragam. Towards interpretable deep generative models via causal representation learning. *Journal of the American Statistical Association*, pages 1–32, 2026. [Cited on p. 1 and 16.]
- [30] J. Pearl. *Probabilistic Reasoning in Intelligent Systems: Networks of Plausible Inference*. Morgan Kaufmann, 1988. [Cited on p. 6.]
- [31] J. Pearl. *Causality*. Cambridge University Press, 9 2009. [Cited on p. 3 and 6.]
- [32] R. Perry, J. von Kügelgen, and B. Schölkopf. Causal discovery in heterogeneous environments under the sparse mechanism shift hypothesis. In *Advances in Neural Information Processing Systems*, volume 35, pages 10904–10917, 2022. [Cited on p. 1.]
- [33] J. Peters, P. Bühlmann, and N. Meinshausen. Causal inference by using invariant prediction: identification and confidence intervals. *Journal of the Royal Statistical Society Series B: Statistical Methodology*, 78(5): 947–1012, 2016. [Cited on p. 1.]
- [34] J. Peters, D. Janzing, and B. Schölkopf. *Elements of Causal Inference: Foundations and Learning Algorithms*. MIT Press, 6 2017. [Cited on p. 3.]
- [35] R. Ranganath, S. Gerrish, and D. Blei. Black box variational inference. In *Artificial Intelligence and Statistics*, pages 814–822. PMLR, 2014. [Cited on p. 7.]
- [36] P. Reizinger, L. Gresele, J. Brady, J. von Kügelgen, D. Zietlow, B. Schölkopf, G. Martius, W. Brendel, and M. Besserve. Embrace the gap: VAEs perform independent mechanism analysis. In *Advances in Neural Information Processing Systems*, volume 35, pages 12040–12057, 2022. [Cited on p. 5.]
- [37] D. J. Rezende, S. Mohamed, and D. Wierstra. Stochastic backpropagation and approximate inference in deep generative models. In *International Conference on Machine Learning*, pages 1278–1286. PMLR, 2014. [Cited on p. 7.]
- [38] H. Robbins. An empirical Bayes approach to statistics. In *Proceedings of the 3rd Berkeley Symposium on Mathematical Statistics and Probability*, pages 157–163, 1956. [Cited on p. 1, 2, 3, and 4.]
- [39] B. Schölkopf and A. J. Smola. *Learning with Kernels: Support Vector Machines, Regularization, Optimization, and Beyond*. MIT press, 2002. [Cited on p. 1.]

- [40] X. Shen, P. Bühlmann, and A. Taeb. Causality-oriented robustness: exploiting general noise interventions in linear structural causal models. *Journal of the American Statistical Association*, 2025. [Cited on p. 15.]
- [41] K. Sohn, H. Lee, and X. Yan. Learning structured output representation using deep conditional generative models. In *Advances in neural information processing systems*, volume 28, 2015. [Cited on p. 7.]
- [42] J. A. Soloff, A. Guntuboyina, and B. Sen. Multivariate, heteroscedastic empirical Bayes via nonparametric maximum likelihood. *Journal of the Royal Statistical Society Series B: Statistical Methodology*, 87(1):1–32, 2025. [Cited on p. 4.]
- [43] Y. Song and S. Ermon. Generative modeling by estimating gradients of the data distribution. In *Advances in neural information processing systems*, volume 32, 2019. [Cited on p. 5.]
- [44] C. Squires, A. Seigal, S. S. Bhate, and C. Uhler. Linear causal disentanglement via interventions. In *International Conference on Machine Learning*, pages 32540–32560. PMLR, 2023. [Cited on p. 1 and 16.]
- [45] M. E. Tipping and C. M. Bishop. Probabilistic principal component analysis. *Journal of the Royal Statistical Society Series B: Statistical Methodology*, 61, 1999. [Cited on p. 3 and 7.]
- [46] J. Tomczak and M. Welling. VAE with a VampPrior. In *International Conference on Artificial Intelligence and Statistics*, pages 1214–1223. PMLR, 2018. [Cited on p. 7.]
- [47] A. B. Tsybakov. *Introduction to Nonparametric Estimation*. Springer Series in Statistics. Springer, New York, 2009. Revised and extended from the 2004 French original, Translated by Vladimir Zaiats. [Cited on p. 7 and 14.]
- [48] B. Varici, E. Acartürk, K. Shanmugam, and A. Tajer. General identifiability and achievability for causal representation learning. In *International Conference on Artificial Intelligence and Statistics*, pages 2314–2322. PMLR, 2024. [Cited on p. 16.]
- [49] B. Varici, E. Acarturk, K. Shanmugam, A. Kumar, and A. Tajer. Score-based causal representation learning: Linear and general transformations. *Journal of Machine Learning Research*, 26(112):1–90, 2025. [Cited on p. 1 and 16.]
- [50] J. von Kügelgen. *Identifiable Causal Representation Learning: Unsupervised, Multi-View, and Multi-Environment*. PhD thesis, University of Cambridge, 2024. [Cited on p. 1.]
- [51] J. von Kügelgen, M. Besserve, L. Wendong, L. Gresele, A. Kekić, E. Bareinboim, D. Blei, and B. Schölkopf. Nonparametric identifiability of causal representations from unknown interventions. In *Advances in Neural Information Processing Systems*, volume 36, pages 48603–48638, 2023. [Cited on p. 1, 7, and 16.]
- [52] J. von Kügelgen, J. Ketterer, X. Shen, N. Meinshausen, and J. Peters. Representation learning for distributional perturbation extrapolation. *arXiv preprint arXiv:2504.18522*, 2025. [Cited on p. 7.]
- [53] M. J. Wainwright and M. I. Jordan. Graphical models, exponential families, and variational inference. *Foundations and Trends® in Machine Learning*, 1(1–2): 1–305, 2008. [Cited on p. 12.]
- [54] L. Wendong, A. Kekić, J. von Kügelgen, S. Buchholz, M. Besserve, L. Gresele, and B. Schölkopf. Causal component analysis. In *Advances in Neural Information Processing Systems*, volume 36, pages 32481–32520, 2023. [Cited on p. 1 and 16.]
- [55] B. Wu, E. N. Weinstein, and D. M. Blei. Bayesian empirical Bayes: Simultaneous inference from probabilistic symmetries. *arXiv preprint arXiv:2512.16239*, 2025. [Cited on p. 1.]
- [56] M. Yang, F. Liu, Z. Chen, X. Shen, J. Hao, and J. Wang. Causalvae: Disentangled representation learning via neural structural causal models. In *Proceedings of the IEEE/CVF conference on computer vision and pattern recognition*, pages 9593–9602, 2021. [Cited on p. 7.]
- [57] D. Yao, D. Rancati, R. Cadei, M. Fumero, and F. Locatello. Unifying causal representation learning with the invariance principle. In *International Conference on Learning Representations*, 2025. [Cited on p. 1, 15, and 16.]
- [58] J. Zhang, K. Greenewald, C. Squires, A. Srivastava, K. Shanmugam, and C. Uhler. Identifiability guarantees for causal disentanglement from soft interventions. In *Advances in Neural Information Processing Systems*, volume 36, 2024. [Cited on p. 1 and 7.]
- [59] K. Zhang, S. Xie, I. Ng, and Y. Zheng. Causal representation learning from multiple distributions: a general setting. In *International Conference on Machine Learning*, pages 60057–60075, 2024. [Cited on p. 1.]

Supplementary Material

Bohan Wu¹

Julius von Kügelgen²

David M. Blei¹

¹ Department of Statistics, Columbia University, USA

² Seminar for Statistics, ETH Zürich, Switzerland

A DETAILS OF THE f -MODELING ALGORITHM

In this appendix, we fill in the detailed derivation of Alg. 1. The full procedure is a variational EM algorithm [53].

The marginal likelihood of (\mathbf{A}, σ^2) is

$$\sum_{e=1}^M \sum_{i=1}^{N_e} \log p_{\mathbf{A}, \sigma^2}^*(\mathbf{x}_{ei} | \mathbf{a}_e) = \sum_{e=1}^M \sum_{i=1}^{N_e} \log \int_{\mathbb{R}^{d_Z}} p_{\mathbf{A}, \sigma^2}(\mathbf{x}_{ei} | \mathbf{z}) p^*(\mathbf{z} | \mathbf{a}_e) d\mathbf{z}.$$

The log-likelihood is difficult to optimize because it involves intractable integrals, so we approximate it using variational inference. In the E-step, we lower bound the log-likelihood by an ELBO. For any $q_{ei} \in \mathcal{P}(\mathbb{R}^{d_Z})$,

$$\begin{aligned} \log p_{\mathbf{A}, \sigma^2}^*(\mathbf{x}_{ei} | \mathbf{a}_e) &\geq \mathbb{E}_{q_{ei}(\mathbf{z}_{ei})} [\log p_{\mathbf{A}, \sigma^2}(\mathbf{x}_{ei} | \mathbf{z}_{ei})] - D_{\text{KL}}(q_{ei}(\mathbf{z}_{ei}) \| p^*(\mathbf{z} | \mathbf{a}_e)) \\ &= -\frac{1}{2\sigma^2} \mathbb{E}_{q_{ei}(\mathbf{z}_{ei})} [\|\mathbf{x}_{ei} - \mathbf{A}\mathbf{z}_{ei}\|^2] - \frac{d_X}{2} \log \sigma^2 - D_{\text{KL}}(q_{ei}(\mathbf{z}_{ei}) \| p^*(\mathbf{z} | \mathbf{a}_e)) \\ &= -\frac{1}{2\sigma^2} \mathbb{E}_{q_{ei}(\mathbf{z}_{ei})} [\|\mathbf{x}_{ei}\|^2 + \mathbf{z}_{ei}^\top \mathbf{D}^2 \mathbf{z}_{ei} - 2\mathbf{x}_{ei}^\top \mathbf{A}\mathbf{z}_{ei}] - \frac{d_X}{2} \log \sigma^2 - D_{\text{KL}}(q_{ei}(\mathbf{z}_{ei}) \| p^*(\mathbf{z} | \mathbf{a}_e)) \\ &=: \text{ELBO}^*(q_{ei}, \mathbf{A}, \sigma^2). \end{aligned}$$

Then we design an EM algorithm which aims to iteratively maximize the objective $\sum_{e=1}^M \sum_{i=1}^{N_e} \text{ELBO}^*(q_{ei}, \mathbf{A}, \sigma^2)$.

Update \mathbf{z} : For given \mathbf{A} and σ^2 , the distribution q_{ei} that maximizes the ELBO is the posterior

$$q_{ei}^*(\mathbf{z}_{ei}) \propto p_{\mathbf{A}, \sigma^2}(\mathbf{x}_{ei} | \mathbf{z}_{ei}) p^*(\mathbf{z}_{ei} | \mathbf{a}_e).$$

A direct calculation shows that, for updating \mathbf{A} and σ^2 in the subsequent M-step, it suffices to keep track of the first and second moments of q_{ei}^* . To approximate these moments, we use the first- and second-order Tweedie formulas.

The score-matching problem can be expressed in terms of the diagonal score components $(\hat{s}_j)_{j \in [d_Z]}$:

$$\hat{s}_j \in \arg \min_{s_j} \sum_{e=1}^M \sum_{i=1}^{N_e} \left[\partial_j s_j \left(y_{eij}, y_{eip_a(j)}, \mathbf{a}_e \right) + \frac{1}{2} s_j \left(y_{eij}, y_{eip_a(j)}, \mathbf{a}_e \right)^2 \right]. \quad (\text{A.1})$$

The resulting score estimate is given by $[\hat{s}(\mathbf{y}, \mathbf{a})]_j = \hat{s}_j(\mathbf{y}_j, \mathbf{y}_{p_a(j)}, \mathbf{a})$, or, under the sparse-intervention approximation, $[\hat{s}(\mathbf{y}, \mathbf{a})]_j = \hat{s}_j(\mathbf{y}_j, \mathbf{y}_{p_a(j)}, \mathbf{a}_j)$, for $j \in [d_Z]$.

Given an estimate \hat{D} of the diagonal matrix D , we update the empirical Bayes estimate of the latent variable \mathbf{z}_{ei} using a damped version of Tweedie's formula:

$$\hat{\mathbf{z}}_{ei} = \hat{D}^{-1} \left(\mathbf{y}_{ei} + \eta \sigma^2 \hat{s}(\mathbf{y}_{ei}, \mathbf{a}_e) \right),$$

where $\eta \in (0, 1)$ is a damping factor.

The second-order Tweedie's formula yields

$$\widehat{z}_{eij}^2 = \widehat{z}_{eij}^2 + \frac{\widehat{\sigma}^2}{\widehat{D}_{jj}^2} + \frac{\widehat{\sigma}^4}{\widehat{D}_{jj}^2} \partial_j \widehat{s}_j(y_j, \mathbf{y}_{\text{pa}(j)}, \mathbf{a}_e), \quad j \in [d_Z].$$

Update A: In the M-step, we maximize the ELBO over \mathbf{A} , equivalently

$$\widehat{\mathbf{A}} = \arg \min_{\mathbf{A} \text{ orthogonal}} \sum_{e=1}^M \sum_{i=1}^{N_e} \mathbb{E}_{\mathbf{q}(\mathbf{z}_{ei})} \left[\mathbf{z}_{ei}^\top \mathbf{D}^2 \mathbf{z}_{ei} - 2 \mathbf{x}_{ei}^\top \mathbf{A} \mathbf{z}_{ei} \right]. \quad (\text{A.2})$$

This optimization depends on the posterior mean and second moments under \mathbf{q} . A natural choice is to take $\mathbb{E}_{\mathbf{q}}[\mathbf{z}_{ei}]$ as the Tweedie estimate $\widehat{\mathbf{z}}_{ei}$, and $\mathbb{E}_{\mathbf{q}}[\mathbf{z}_{ei}^2] \in \mathbb{R}^{d_Z}$ as the second-order Tweedie estimate $\widehat{\mathbf{z}}_{ei}^2$.

Define $\mathbf{M} := \sum_{e=1}^M \sum_{i=1}^{N_e} \mathbf{x}_{ei} \widehat{\mathbf{z}}_{ei}^\top$. The optimization problem reduces to

$$\begin{aligned} \widehat{\mathbf{A}} &= \arg \min_{\mathbf{A}} \sum_{e=1}^M \sum_{i=1}^{N_e} \left[\sum_{j=1}^{d_Z} \mathbf{D}_{jj}^2 \widehat{z}_{eij}^2 - 2 \langle \mathbf{x}_{ei}, \mathbf{A} \widehat{\mathbf{z}}_{ei} \rangle \right] \\ &= \sum_{e=1}^M \sum_{i=1}^{N_e} \sum_{j=1}^{d_Z} \mathbf{D}_{jj}^2 \widehat{z}_{eij}^2 - 2 \text{tr}(\mathbf{A} \mathbf{M}^\top). \end{aligned} \quad (\text{A.3})$$

where the second equality is due to

$$\sum_{e=1}^M \sum_{i=1}^{N_e} \langle \mathbf{x}_{ei}, \mathbf{A} \widehat{\mathbf{z}}_{ei} \rangle = \sum_{e=1}^M \sum_{i=1}^{N_e} \text{tr}(\mathbf{A} \widehat{\mathbf{z}}_{ei} \mathbf{x}_{ei}^\top) = \text{tr}(\mathbf{A} \mathbf{M}^\top).$$

Now we parametrize $\mathbf{A} = \mathbf{O} \mathbf{D}$ thanks to Thm. 4.1.

Let $\mathbf{M} = \mathbf{U} \mathbf{\Sigma} \mathbf{V}^\top$ be the singular value decomposition of \mathbf{M} . Since the trace is cyclically invariant, the objective (A.3) is equivalent to $\text{tr}(\mathbf{O} \mathbf{D} \mathbf{M}^\top) = \text{tr}(\mathbf{O} \mathbf{V} \mathbf{D} \mathbf{\Sigma}^\top \mathbf{U}^\top)$. By the orthogonal Procrustes solution [16, §6.4.1], for a given \mathbf{D} , the solution $\widehat{\mathbf{O}}$ that maximizes Eq. (A.3) is given by

$$\widehat{\mathbf{O}} = \mathbf{U} \mathbf{V}^\top \in \mathcal{O}^{d_X \times d_Z}.$$

After plugging $\widehat{\mathbf{O}}$ into the reformulated objective, the optimal $\widehat{\mathbf{D}}$ requires solving

$$\begin{aligned} \widehat{\mathbf{D}} &= \arg \min_{\mathbf{D}} \sum_{e=1}^M \sum_{i=1}^{N_e} \sum_{j=1}^{d_Z} \mathbf{D}_{jj}^2 \widehat{z}_{eij}^2 - 2 \text{tr}(\mathbf{U} \mathbf{D} \mathbf{\Sigma}^\top \mathbf{U}^\top) \\ &= \sum_{e=1}^M \sum_{i=1}^{N_e} \sum_{j=1}^{d_Z} \mathbf{D}_{jj}^2 \widehat{z}_{eij}^2 - 2 \text{tr}(\mathbf{D} \mathbf{\Sigma}^\top). \end{aligned}$$

The problem reduces to solving a quadratic function for each entry of \mathbf{D} . The optimizer is explicitly given by $\widehat{D}_{jj} = \mathbf{\Sigma}_{jj} / \sum_{e=1}^M \sum_{i=1}^{N_e} \widehat{z}_{eij}^2$ for $j \in [d_Z]$.

Update σ^2 . Finally, we freeze $\{\widehat{\mathbf{z}}_{ei}\}$, $\{\widehat{\mathbf{z}}_{ei}^2\}$, and $\widehat{\mathbf{A}}$, and maximize the ELBO with respect to σ^2 . The ELBO is concave in $1/\sigma^2$, so setting the derivative to zero yields the unique maximizer

$$\widehat{\sigma}^2 = \frac{1}{d_X \sum_{e=1}^M N_e} \sum_{e=1}^M \sum_{i=1}^{N_e} \left(\|\mathbf{x}_{ei}\|_2^2 + \sum_{j=1}^{d_Z} \widehat{D}_{jj}^2 \widehat{z}_{eij}^2 - 2 \mathbf{x}_{ei}^\top \widehat{\mathbf{A}} \widehat{\mathbf{z}}_{ei} \right).$$

A.1 SCORE MODELING WITH CUBIC SPLINES

To estimate the diagonal score components $\{s_j\}_{j \in [d_Z]}$, we use a simple spline-based nonparametric model [47] that admits closed-form updates. Fix $j \in [d_Z]$ and let $x_{eij} := (y_{eij}, y_{eipa(j)}) \in \mathbb{R}^{|\text{pa}(j)|+1}$ denote the input. We model

$$s_j(y_{eij}, y_{eipa(j)}, a_{ej}) = \phi_j(x_{eij})^\top \theta_{j,a_{ej}},$$

where $\phi_j : \mathbb{R}^{|\text{pa}(j)|+1} \rightarrow \mathbb{R}^m$ is a tensor-product cubic B-spline feature map with a fixed knot sequence on each coordinate, and $\theta_{j,a} \in \mathbb{R}^m$ are intervention-specific coefficients for $a \in \{0, 1\}$. In particular, if we use K basis functions per coordinate, then the tensor-product construction yields $m = K^{|\text{pa}(j)|+1}$ features, so both memory and computational complexity grow exponentially in the input dimension $|\text{pa}(j)| + 1$.

Write $\Psi_j(x) := \partial_{y_j} \phi_j(x) \in \mathbb{R}^m$ for the derivative of the spline features with respect to the first coordinate y_j . Then

$$\partial_{y_j} s_j(y_{eij}, y_{eipa(j)}, a_{ej}) = \Psi_j(x_{eij})^\top \theta_{j,a_{ej}}.$$

Plugging this parameterization into the empirical score-matching loss for the j th component yields the quadratic objective

$$\widehat{\mathbf{L}}_j(\theta_{j0}, \theta_{j1}) = \frac{1}{M} \sum_{e=1}^M \frac{1}{N_e} \sum_{i=1}^{N_e} \left\{ \Psi_j(x_{eij})^\top \theta_{j,a_{ej}} + \frac{1}{2} (\phi_j(x_{eij})^\top \theta_{j,a_{ej}})^2 \right\}.$$

We fit θ_{j0}, θ_{j1} with ridge regularization,

$$(\widehat{\theta}_{j0}, \widehat{\theta}_{j1}) \in \arg \min_{\theta_{j0}, \theta_{j1}} \widehat{\mathbf{L}}_j(\theta_{j0}, \theta_{j1}) + \frac{\lambda}{2} (\|\theta_{j0}\|_2^2 + \|\theta_{j1}\|_2^2),$$

which decouples over $a \in \{0, 1\}$. For each a , define the index set $\mathcal{I}_{ja} := \{(e, i) : a_{ej} = a\}$, the feature and derivative matrices

$$\Phi_{ja} \in \mathbb{R}^{|\mathcal{I}_{ja}| \times m}, \quad \Phi_{ja}(r, :) = \phi_j(x_{eij})^\top, \quad \Psi_{ja} \in \mathbb{R}^{|\mathcal{I}_{ja}| \times m}, \quad \Psi_{ja}(r, :) = \Psi_j(x_{eij})^\top,$$

and the normal equations

$$\widehat{\theta}_{ja} = - \left(\Phi_{ja}^\top \Phi_{ja} + \lambda I_m \right)^{-1} \Psi_{ja}^\top \mathbf{1}.$$

The resulting score estimator is $\widehat{s}_j(x, a) = \phi_j(x)^\top \widehat{\theta}_{ja}$, and $\partial_{y_j} \widehat{s}_j(x, a) = \Psi_j(x)^\top \widehat{\theta}_{ja}$, which are the quantities used in the first- and second-order Tweedie updates.

A.2 ADDRESSING SCALE-PERMUTATION INDETERMINACY

From the objective (4.7), the columns of \mathbf{A} are identifiable only up to signed permutations. Specifically, if \mathbf{D}_{sign} be a diagonal matrix with entries in $\{\pm 1\}$ and \mathbf{P} a permutation matrix, then objective (4.7) remains unchanged if we replace \mathbf{D} with $\mathbf{D}\mathbf{D}_{\text{sign}}$ and \mathbf{O} with $\mathbf{P}\mathbf{O}$. To obtain more stable updates, we select a canonical representative by replacing step (4.8) with $\widehat{\mathbf{A}} = \mathbf{U}\mathbf{P}\mathbf{V}^\top \mathbf{D}_{\text{sign}} \mathbf{D}$, where \mathbf{P} is the permutation matrix that maximizes $\sum_{j=1}^{d_Z} |(\mathbf{P}\boldsymbol{\Sigma})_{jj}|$ and $\mathbf{D}_{\text{sign}} = \text{sign}(\boldsymbol{\Sigma})$.

A.3 JUSTIFYING THE SPARSE INTERVENTION APPROXIMATION

The sparse intervention approximation becomes accurate in the large-sample regime. By Bayes' rule, we have

$$f_{\mathbf{a}_e}(y_j | \mathbf{y}_{\text{pa}(j)}) = \int_{\mathbb{R}^{|\text{pa}(j)|+1}} \text{p}(y_j | z_j) \text{p}_{a_{ej}}(z_j | z_{\text{pa}(j)}) \text{p}_{\mathbf{a}_e}(z_{\text{pa}(j)} | \mathbf{y}_{\text{pa}(j)}) \text{d}z_{\text{pa}(j) \cup \{j\}}. \quad (\text{A.4})$$

As we observe samples $\{\mathbf{y}_{eipa(j)}\}_{i=1}^{N_e}$, when N_e is large, the posterior $\text{p}_{\mathbf{a}_e}(z_{\text{pa}(j)} | \mathbf{y}_{\text{pa}(j)})$ which is invariant across i centers around the distribution

$$\widehat{\text{p}}(z_{\text{pa}(j)} | \mathbf{y}_{\text{pa}(j)}) \propto \text{p}(\mathbf{y}_{\text{pa}(j)} | \widehat{z}_{\text{pa}(j)}) \widehat{\mathbf{g}}(z_{\text{pa}(j)})$$

where $\widehat{\mathbf{g}}$ is the empirical distribution of the denoised estimates $\{\widehat{z}_{eipa(j)}\}_{i=1}^{N_e}$ learned from the normal means model. This substitute yields the approximation

$$f_{\mathbf{a}_e}(y_j | \mathbf{y}_{\text{pa}(j)}) \approx \int_{\mathbb{R}^{|\text{pa}(j)|+1}} \text{p}(y_j | z_j) \text{p}_{a_{ej}}(z_j | z_{\text{pa}(j)}) \widehat{\text{p}}(z_{\text{pa}(j)} | \mathbf{y}_{\text{pa}(j)}) \text{d}z_{\text{pa}(j) \cup \{j\}} =: f_{a_{ej}}(y_j | \mathbf{y}_{\text{pa}(j)}),$$

thus asymptotically the conditional density depends on the environment only through the local intervention indicator a_{ej} . Thus, the constraint to depend on a_j can be viewed as a causal invariance constraint that requires \mathbf{y} to act in a sparse way given the intervention \mathbf{a} [57].

B PROOF OF THM. 5.1

Theorem 5.1. *For all solutions $s^* \in \arg \min_{s \in \mathcal{S}} \mathbf{L}^{\mathcal{G}}(s)$ and all $j \in [d_Z]$, the j^{th} component s_j^* of s^* minimizes*

$$\sum_{e=1}^M \mathbb{E}_{\mathbf{y} \sim f_{\mathbf{a}_e}} \left[\left| s_j \left(y_j, \mathbf{y}_{\text{pa}(j)}, a_{ej} \right) \right|^2 + 2 \partial_j s_j \left(y_j, \mathbf{y}_{\text{pa}(j)}, a_{ej} \right) \right]. \quad (\text{B.1})$$

Proof. Hyvärinen and Dayan [18, Theorem 1] shows that

$$\mathbf{L}^{\mathcal{G}}(s) = \sum_{e=1}^M \mathbb{E}_{\mathbf{y} \sim f_{\mathbf{a}_e}^{\mathcal{G}}} \left[\left\| s(\mathbf{y}, \mathbf{a}_e) \right\|^2 + 2 \text{tr}(\nabla_{\mathbf{y}} s(\mathbf{y}, \mathbf{a}_e)) + \left\| s^{\mathcal{G}}(\mathbf{y}, \mathbf{a}_e) \right\|^2 \right]. \quad (\text{B.1})$$

The last term in (B.1) does not depend on s and can be dropped. Hence, minimizing $\mathbf{L}^{\mathcal{G}}(s)$ is equivalent to minimizing

$$\sum_{e=1}^M \mathbb{E}_{\mathbf{y} \sim f_{\mathbf{a}_e}^{\mathcal{G}}} \left[\left\| s(\mathbf{y}, \mathbf{a}_e) \right\|^2 + 2 \text{tr}(\nabla_{\mathbf{y}} s(\mathbf{y}, \mathbf{a}_e)) \right]. \quad (\text{B.2})$$

Using the structure (5.2), we can rewrite (B.2) as

$$s \mapsto \sum_{e=1}^M \sum_{j=1}^{d_Z} \mathbb{E}_{\mathbf{y} \sim f_{\mathbf{a}_e}^{\mathcal{G}}} \left[\left| s_j \left(y_k, \mathbf{y}_{\text{pa}(k)}, \mathbf{a}_e \right) \right|^2 + 2 \partial_j s_j \left(y_j, \mathbf{y}_{\text{pa}(j)}, \mathbf{a}_e \right) \right]. \quad (\text{B.3})$$

□

C WEIGHTED f -MODELING CRL

The current method assigns uniform importance to each environment in the objective. However it is often desirable to learn a causal model that prioritizes accuracy in certain environments over others. For example, the base environment $\mathbf{a} = 0$ may be of particular interest. To account for such preferences, we could consider the weighted score-matching objective:

$$\hat{s} = \arg \min_{s \in \mathcal{S}} \sum_{e=1}^M w_e \sum_{i=1}^{N_e} \sum_{j=1}^{d_Z} \left[\partial_j [s(\mathbf{y}_{ei}, \mathbf{a}_e)]_j + \frac{1}{2} ([s(\mathbf{y}_{ei}, \mathbf{a}_e)]_j)^2 \right],$$

where $w_e \geq 0$ denotes the weight assigned to environment e , subject to $\sum_{e=1}^M w_e = 1$. The weights determine the relative influence of each environment on the score matching loss. Higher w_e assign more importance to environment e .

In the absence of prior information or labeled test data, one may choose uniform weights $w_e = 1/M$, or alternatively set w_e proportional to the sample size N_e to account for imbalance across environments. If a particular environment (e.g., the base SCM with $\mathbf{a}_e = 0$) is of interest, one may assign it a dominant weight (e.g., $w_e \approx 1$) and downweight the others accordingly. Other methods for choosing the environment weights are discussed [40].

D DETAILS OF THE EMPIRICAL STUDY

In all experiments, we run CRL f -modeling (Alg. 1) for 1,000 iterations on an H100 GPU. We set $\eta = 1$ when using empirical Bayes shrinkage, parameterize each s_j by cubic splines with 8 knots on $[-15, 15]$, and initialize \mathbf{A} using the PCA loading matrix.

In the first experiment (left column of Fig. 3), we simulate 40 independent runs of the specified causal model by drawing \mathbf{A}^* and σ^{2*} anew in each run. In each run, we generate $N_e = 2,000$ samples for each single-node intervention target.

In the last experiment (right column of Fig. 3), we simulate $M = 20$ single-node interventions under a fixed specification $(\mathbf{A}^*, \sigma^{2*})$, with 4 environments per intervention and $N_e = 500$ samples per environment.

E IDENTIFICATION THEORY

In this section, we review identifiability results of the latent variables \mathbf{z} in CRL, with an emphasis on the linear measurement model with nonlinear latent causal model. Denote a generic estimator $\hat{\mathbf{z}}$ given \mathbf{x} by $\hat{\mathbf{z}}(\mathbf{x}) : \mathbb{R}^{d_x} \mapsto \mathbb{R}^{d_z}$.

In representation learning, point identification is typically unattainable; instead, one often aims for set identification or identification up to an equivalence class [2, 29, 57]. Identification results can be algorithm-agnostic and do not require a specific method to recover the parameters. The working model (3.1) corresponds to the setting of causal representation learning (CRL) with a linear measurement model, a general SCM, and known causal DAG and intervention targets. We now review some useful notions of identifiability to discuss our results.

Definition E.1 (Element-identifiability / Disentanglement). A learned representation $\hat{\mathbf{z}} \in \mathbb{R}^{d_z}$ is said to be *element-identifiable* if there exists a permutation matrix $\mathbf{P}_\pi \in \mathbb{R}^{d_z \times d_z}$ and an element-wise diffeomorphism $h(\mathbf{z}) := (h_1(z_1), \dots, h_{d_z}(z_{d_z})) \in \mathbb{R}^{d_z}$ such that

$$\hat{\mathbf{z}} = \mathbf{P}_\pi h(\mathbf{z}^*). \quad (\text{E.1})$$

Element-identifiability is also known as *perfect latent recovery* in the language of Varici et al. [48], where a representation $\hat{\mathbf{z}}$ satisfying this condition is said to be *perfect*. It is also referred to as *disentanglement* in the sense of Moran and Aragam [29, Definition 5].

Definition E.2 (Scale-permutation-identifiability). A learned representation $\hat{\mathbf{z}} \in \mathbb{R}^{d_z}$ is said to be *scale-permutation-identifiable* if there exists a permutation matrix $\mathbf{P}_\pi \in \mathbb{R}^{d_z \times d_z}$ and a diagonal sign matrix $\mathbf{D} \in \mathbb{R}^{d_z \times d_z}$ such that

$$\hat{\mathbf{z}} = \mathbf{P}_\pi \mathbf{D} \mathbf{z}^*. \quad (\text{E.2})$$

Scale-permutation-identifiability is a stronger form of element-identifiability. It describes recovery of the ground-truth latent variables up to permutation and rescaling, which are common forms of ambiguities in linear latent variable models.

Definition E.3 (Mixing-identifiability). A learned representation $\hat{\mathbf{z}} \in \mathbb{R}^{d_z}$ is said to be *mixing-identifiable* if there exists a permutation matrix $\mathbf{P}_\pi \in \mathbb{R}^{d_z \times d_z}$, a diagonal matrix $\mathbf{D} \in \mathbb{R}^{d_z \times d_z}$ and sparse matrix $\mathbf{C} \in \mathbb{R}^{d_z \times d_z}$ satisfying that $\mathbf{C}_{jj} = 0$ for all $j \in [d_z]$ and

$$\text{ch}(i) \not\subseteq \text{ch}(j) \implies \mathbf{C}_{ij} = 0, \forall i \in [d_z],$$

such that $\hat{\mathbf{z}} = \mathbf{P}_\pi (\mathbf{D} + \mathbf{C}) \mathbf{z}^*$.

This condition ensures that $\hat{\mathbf{z}}$ is constrained by the causal graph structure, where mixing occurs only among variables with nested parent sets.

There has been extensive recent work on the question of identifiability in CRL. Under Thm. 3.1, identifiability typically holds only up to an equivalence class determined by the available interventions; for example, Squires et al. [44] establish such results under a linear measurement model together with a *linear* latent SCM. Several works clarify the limits and possibilities of identifiability. Under hard interventions and a linear measurement model, Squires et al. [44, Prop. 2] and Buchholz et al. [7, Remark 2] show that latent variables are identifiable only up to scaling and permutation, and that this is optimal without further assumptions on the causal variables \mathbf{z} . For stochastic interventions, Varici et al. [49, Thm. 14] show that under soft interventions and Thm. 3.1, one can identify latent variables up to mixing with their parents and recover the DAG up to transitive closure; moreover, if each node receives one hard intervention, then under a linear latent SCM both the DAG and the latent variables are identifiable (up to scaling) [49, Thm. 16]. For general latent SCMs under soft interventions, Varici et al. [49, Thm. 18] show that intervening on each node at least once suffices to recover the latent variables up to parent mixing. Beyond linear SCMs, Jin and Syrgkanis [23, Thm. 3] establish recovery guarantees for general nonparametric SCMs via score-matching objectives, identifying latents up to componentwise monotone transformations under suitable conditions. In the fully nonparametric measurement setting, von Kügelgen et al. [51] provide identifiability guarantees (and impossibility results) showing that element-identifiability in the sense of Thm. E.1 is the sharp guarantee in general, even when one perfect intervention per node is available.

We refer to Varici et al. [49] for a comprehensive study of identifiability results for multi-domain CRL across linear and nonparametric models and a range of interventional designs. We emphasize, however, that most of the aforementioned CRL identifiability theory does *not* assume the causal graph (or intervention targets) to be known, whereas our approach requires the true causal graph and intervention targets as inputs. This regime is studied in the setting of causal component analysis [54], who establish identifiability results for several classes of interventions in the known-graph setting.